Published in final edited form as:

Cancer Immunol Res. 2019 March ; 7(3): 428–442. doi:10.1158/2326-6066.CIR-18-0061.

A CD40 agonist and PD-1 antagonist antibody reprogram the microenvironment of non-immunogenic tumors to allow T cell–mediated anticancer activity

Hayley S. Ma[1], **Bibhav Poudel**[1], **Evanthia Roussos Torres**[1], **John-William Sidhom**[1], **Tara M. Robinson**[1], **Brian Christmas**[1], **Blake Scott**[1], **Kayla Cruz**[1], **Skylar Woolman**[1], **Valerie Z. Wall**[2], **Todd Armstrong**[1], and **Elizabeth M. Jaffee**[1]

[1]Dept of Oncology, Viragh Center for Pancreatic Clinical Research and Care, Bloomberg Kimmel Institute for Immunotherapy, and the Sidney Kimmel Cancer Center at Johns Hopkins University School of Medicine, Baltimore, MD 21205, USA

[2]Benaroya Research Institute at Virginia Mason, Seattle, WA

Abstract

In cancers with tumor infiltrating lymphocytes (TIL), monoclonal antibodies (mAbs) that block immune checkpoints such as CTLA-4 and PD-1/PD-L1 promote antitumor T cell immunity. Unfortunately most cancers fail to respond to single agent immunotherapies. T regulatory cells, myeloid derived suppressor cells (MDSCs), and extensive stromal networks within the tumor microenvironment (TME) dampen antitumor immune responses by preventing T-cell infiltration and/or activation. Few studies have explored combinations of immune checkpoint antibodies that target multiple suppressive cell populations within the TME, and fewer have studied the combinations of both agonist and antagonist mAbs on changes within the TME. Here we test the hypothesis that combining a T cell–inducing vaccine with both a PD-1 antagonist and CD40 agonist mAbs (triple therapy) will induce T cell priming and TIL activation in mouse models of non-immunogenic solid malignancies. In an orthotopic breast cancer model and both subcutaneous and metastatic pancreatic cancer mouse models, only triple therapy was able to eradicate most tumors. The survival benefit was accompanied by significant tumor infiltration of IFNγ-, Granzyme B-, and TNFα-secreting effector T cells. Further characterization of immune populations was carried out by high dimensional flow cytometric clustering analysis and visualized by t-distributed stochastic neighbor embedding (t-SNE). Triple therapy also resulted in increased infiltration of dendritic cells, maturation of antigen presenting cells, and a significant decrease in granulocytic MDSCs. These studies reveal that combination CD40 agonist and PD-1 antagonist mAbs reprogram immune resistant tumors in favor of antitumor immunity.

Keywords

Cancer vaccines; antibody immunotherapy; tumor microenvironment; breast cancer; pancreatic cancer

Corresponding Author: Elizabeth M. Jaffee, M.D. ejaffee@jhmi.edu, 1650 Orleans St, CRB1 Room 4M07, Baltimore, MD 21287. Tel: 410-955-2957; Fax: 410-664-8216.

INTRODUCTION

Development of T cell immune checkpoint inhibitors (ICIs) that block the programmed death 1 (PD-1) pathway have led to substantial responses in several tumor types (1–4). However, these responses are limited to cancers primed for antitumor immunity. Tumors responsive to anti–PD-1 therapy are likely hypermutated, highly infiltrated with effector T cells, and highly express PD-1 ligand (PD-L1) on tumor cells within the tumor microenvironment (TME) (5). However, most tumors develop strategies to evade immune surveillance, leading to immune tolerance, a major obstacle in implementation of successful immunotherapy (6). The majority of immune suppression mechanisms suppress effector T cell infiltration and function in the TME. These include T regulatory cells (Tregs), myeloid derived suppressor cells (MDSCs), tumor associated macrophages (TAM), immature dendritic cells (DCs), and an extensive stromal network of cells and signals that prevent T-cell infiltration (7,8). Many tumors also fail to elicit antigen-specific T cell responses due to early tumor immune evasion mechanisms or lack of tumor immunogenicity (9).

Most pancreatic adenocarcinomas (PDAC) and breast cancers have multiple immune suppressive cell populations in their TME, including monocytic subpopulations and immature DCs (10–12). The majority of patients with these cancers fail to mount an effector T cell response capable of recognizing cancer cells. Preclinical studies report substantial synergism in combining cancer vaccines with ICIs (13–17). However, few clinical trials have demonstrated benefit (18–21). We previously reported that a human PDAC vaccine alone or in combination with the ICI, ipilimumab, promoted development of lymphoid aggregates and led to transient antigen-specific T cell responses associated with short-term increases in survival (22,23). Repeated antigen stimulation in the absence of durable antigen presentation and/or appropriate costimulatory signals may lead to T cell exhaustion and/or anergy and tolerance. However, if the proper signal is provided to APCs for continued T cell activation, it should lead to more durable responses. A few studies have begun to test agonist immune-oncology (I-O) mAbs that target costimulatory pathways such as anti-CD40, anti–OX-40, and anti-CD137, either alone or in combination with either chemotherapy or ICIs (24–29). CD40, a tumor necrosis factor (TNF) receptor superfamily member, is expressed on many immune cell types, including DCs, macrophages, B cells, and NK cells (30). CD40 signaling induced by CD40L-expressing T helper (Th1) cells on CD40-expressing antigen presenting cells (APCs) is critical for APC licensing (31). Administration of CD40 agonist mAb upregulates MHCII, CD80, and CD86 on DCs and macrophages (31), can promote $CD8^+$ T cell activation *in vivo* (32), and likely alters the TME myeloid component (25,33). Therapeutic strategies incorporating CD40 pathway stimulation have been successful in preclinical studies in promoting antigen-specific T cell expansion (15,34–36).

Early clinical trials of dacetuzumab, a humanized CD40 mAb, demonstrated responses in hematologic malignancy patients and has entered phase II studies (37). CP870,893, a fully human mAb studied in a number of solid tumors, has shown objective responses in about 20% of melanoma and PDAC patients (27,31). Preclinical studies demonstrated synergy with anti–PD-1 and CD40 mAb (33,38,39) by altering the TME myeloid component, and clinical trials combining CD40 mAb with gemcitabine-based chemotherapy in PDAC are ongoing (25).

We tested the hypothesis that combining a T cell generating vaccine with a CD40 agonist mAb and anti–PD-1 can induce long-term survival by inducing antitumor CTL trafficking into nonimmunogenic solid malignancies. We show that triple therapy can enhance CTL infiltration in the TME in a tolerance model of breast cancer and a metastatic model of PDAC. We also provide evidence that granulocytic MDSCs (G-MDSCs) are reduced and macrophage and dendritic cell populations become mature APCs capable of activating effector $CD8^+$ T cells and Th cells.

MATERIALS AND METHODS

Mice

Male C57BL/6 mice, age 7–8 weeks, were obtained from Jackson Laboratories. Female *neu*-N mice were bred and maintained at the Animal Core Facility at Johns Hopkins University as described previously (40). T cell receptor (TCR) transgenic mice were engineered to express a *neu*-specific TCR and were maintained as described previously (41,42). All mice were housed in microisolator cages in a pathogen-free animal facility. All animal procedures were conducted in accordance with, and with approval of, the policy of the Johns Hopkins University School of Medicine Institutional Animal Care and Use Committee.

Cell Lines

NT2.5 cells are a syngeneic *neu*-expressing mammary tumor cell line derived from the *neu*-N mouse model (42–44). 3T3-neuGM (vaccine) cells are 3T3 cells that have been transfected to constitutively express GM-CSF and HER-2/neu (43,45). Both cell lines were authenticated by flow cytometry to confirm HER-2/neu expression, and the 3T3 cells were confirmed by ELISA to express GM-CSF. $T2D^q$ cells are T2 B lymphoblast/ T lymphoblast hybrid human cells deficient in the MHC-I TAP transporter molecule and engineered to express D^q (46). They were authenticated by sequencing and flow cytometry to confirm HLA-D^q expression. PANC02 mouse pancreatic tumor cells were derived and maintained as previously described (47). The cell line was authenticated by whole exome sequencing for tumor genes and neoantigens. B78H1-GM cells are an MHC class I-negative variant of B16 melanoma cell line engineered to secrete GM-CSF, and authenticated by ELISA (48–50). All cell lines were obtained between 2010 and 2015 and passaged no more than 10 times between thawing and use in experiments. All cell lines were tested for mycoplasma prior to use in experiments (last tested June 2017). *In vitro* stimulation was performed using CTL medium which consisted of RPMI media with 10% FBS, 1% L-glutamine, 0.5% Pen/Strep, and 0.1% 2-mercaptoethanol (Life Technologies).

Reagents and Antibodies

Therapeutic monoclonal antibodies (mAb) were obtained from BioXcell. Anti–PD-1 (clone RMP1–14), anti-CD40 (clone FGK4.5), and rat IgG Isotype (clone 2A3) were administered intraperitoneally (i.p.) at 100 μg in 100 μl phosphate buffered saline (PBS). Anti-CD8α (clone 2.43), anti-CD4 (clone GK1.5) and Isotype (clone LTF-2) were administered i.p. at 200 μg in 100 μl PBS on Day −2, Day 0 and twice weekly thereafter (51,52). Cyclophosphamide (Cy) was obtained from Baxter Healthcare Corp. and prepared as a 20

mg/ml stock solution in water. Any unused solution was discarded after 2 weeks. Mice were administered Cy at 100 mg/kg in 500 μl PBS i.p.

A complete list of fluorescent-conjugated antibodies for flow cytometry can be found in Supplementary Table S1.

In vivo tumor models and therapy

For *neu*-N experiments, 8 week old female mice were inoculated with NT2.5 mammary tumor cells in the right mammary fat pad. 5×10^4 cells were administered on Day −3 for survival studies, whereas 1×10^6 cells were injected on Day −8 for TIL analysis studies to allow for establishment of 5×5 mm tumors prior to treatment (42,53,54). The 3T3neuGM vaccine was irradiated at 50 Gy and three subcutaneous (sc) injections of 10^6 vaccine cells each were given in 100 μl, in the left upper limb and both lower limbs on Day 0 (41–43,48). Cyclophosphamide (Cy, 100 mg/kg i.p. in 500 μl PBS) was given i.p. on Day −1 to all mice receiving vaccine. For survival studies, all mice received 2×10^6 *neu*-specific $CD8^+$ T cells i.v. on Day 1, unless otherwise specified (42,53,54). For TIL and TDLN analysis studies, all mice received 6×10^6 *neu*-specific $CD8^+$ T cells i.v. on Day 1. Anti–PD-1 mAb, CD40 mAb or rat IgG isotype control, was given on Day 2. For TIL studies, all tissues were harvested at Day 6 unless otherwise specified. For survival studies, anti–PD-1 mAb or isotype control mAb was continued twice weekly thereafter. Tumors were measured twice weekly and tumor volume was calculated as follows: Volume = $(L\times W^2)/2$. Mice were euthanized if tumors reached >500 mm^3.

For the PDAC metastatic model, 8 week old male C57BL/6 mice underwent general anesthesia with isofluorane then received 2×10^6 PANC02 cells on Day −15 via intrasplenic injection followed by hemisplenectomy (47,50). A 1:1 mixture of PANC02 and B78H1-GM cells (PANC02vac) was irradiated (50 Gy) and given on Day 0 and Day 14 (50). Cy (100 mg/kg i.p. in 500 μl PBS) was given i.p. on Day −1 to all mice receiving PANC02vac. Anti–PD-1, CD40 and rat IgG isotype mAb were administered per the schedule described for *neu*-N. Livers were harvested for TIL analysis on Day 21. Mice were monitored for survival and considered moribund upon signs of lethargy and/or ascites.

For the PDAC sc model, which allows for early observation of primary tumor growth changes (55,56), mice received 10^6 PANC02 cells sc in the left lower limb on Day −15. PANC02vac, Cy, and mAb therapy were given as described above. Tumors were measured twice weekly and mice were euthanized if tumors reached >500 mm^3.

Tissue processing

Tumors were dissected and chopped into 2×2 mm or smaller fragments and transferred to C-tubes containing 2.5 ml tumor dissociation enzyme solution (Mouse Tumor Dissociation Kit, Miltneyi Biotech). Tubes were processed on an Octo-Dissociator (Miltenyi) using the 37C_mTDK_2 protocol designated for hard tumor tissue. Digested tumors were quenched with 20 ml RPMI containing 10% FBS and 1% Pen/Strep (hereafter referred to as complete media) and passed through 70 μM cell strainers (Falcon). Cells were centrifuged at 350 × g for 10 minutes at 4 °C, aspirated, and red blood cell lysed with 1 ml Ack lysis solution (Quality Biological) for 2 minutes at room temperature (rt). Cells were quenched with 10 ml

complete media, centrifuged, and resuspended in complete media for counting and plating for downstream applications.

Livers were dissected and processed in the same manner as tumors, followed by an additional Percoll isolation step after Ack lysis. Cell suspensions were prepared in 6 ml of 80% Percoll (GE Healthcare) and underlayed with 6 ml 40% Percoll in a 15 ml conical tube. Cells were centrifuged for 25 min at 2400 × g at rt with no brake, and the layer containing mononuclear cells was transferred to a tube containing 30 ml complete media. Cells were centrifuged at 350 × g for 10 min, aspirated, and resuspended in complete media.

Lymph nodes (LN) were dissected and firmly pressed through 40 μM cell strainers with a 3 ml syringe plunger in 5 ml complete media. Cell suspensions were centrifuged at 350 × g for 5 minutes at 4º C and resuspended in complete media.

Spleens were processed in the same manner as LN, with an additional Ack lysis step after the first centrifugation. Cells were quenched in complete media, centrifuged and resuspended in complete media. For adoptive T cell transfer, $CD8^+$ T cells were isolated using the mouse CD8 negative selection kit according to the manufacturer specifications (Stem Cell Technologies), washed twice with PBS, and resuspended in PBS at $1–2\times10^7$/ml for intravenous (i.v.) injection.

In vitro cytokine detection

Cell suspensions isolated from tumors or LN of treated *neu*-N mice were plated in complete media with 50 μM β-mercaptoethanol at 1×10^6 cells/ml media in 24-well tissue culture plates. Antigen presenting cells were prepared by pulsing $T2D^q$ cells for 2–3 hours in CTL media containing 20 mg/ml of $RNEU_{420–429}$ (RNEU, PDSLRDLSVF) or the negative control peptide LCMV $NP_{118–126}$ (NP, PQASGVYM) (42). Peptides were produced in the Johns Hopkins Biosynthesis and Sequence Facility at a purity of 95%. Peptide-pulsed $T2D^q$ cells were washed and plated at a 1:4 ratio with mouse TIL or LN cells in the presence of protein transport inhibitor (GolgiPlug, BD Bioscience). Cells were incubated at 37 °C overnight, followed by intracellular flow cytometry analysis of cytokine expression.

Cell suspensions isolated from livers of treated PANC02 hemispleen mice were plated as described above. Cells were stimulated overnight in the presence of GolgiPlug with CD3/CD28 mouse T cell activation beads (Gibco) according to manufacturer specifications. The following day, cells were resuspended with vigorous pipetting, transferred to 1 ml eppendorf tubes, and separated from activation beads under magnetic isolation. Cells were centrifuged at 350 × g for 5 minutes and plated for intracellular flow cytometry analysis of cytokine expression.

Flow cytometry

Freshly harvested mouse cells were plated in 96-well U-bottom plates (up to 2×10^6/well) in PBS. Cells were stained with Live/Dead near-IR stain (Invitrogen) for 30 minutes, followed by a 30 minute incubation in a cocktail of surface antibodies (target and isotype control cocktails) prepared in FACS buffer (1X HBSS with 2% FCS, 0.1% sodium azide and 0.1% HEPES). For intracellular staining, cells were permeablized with the FoxP3 transcription

factor staining buffer kit (Invitrogen) according to manufacturer specifications. Cells were then incubated in a cocktail of intracellular antibodies (target and isotype cocktails) prepared in 1X perm wash buffer for 30 minutes, and washed twice in perm wash buffer prior to data collection. Fluorescence acquisition was carried out on a Beckman Coulter Gallios flow cytometer and analyzed on FlowJo v10.1 (TreeStar).

Clustering Analysis and t-SNE Visualization

Clustering analysis was performed in order to analyze and visualize the high-dimensional nature of our flow cytometry data. First we applied fsc/ssc and live/dead gating, then $CD8^+$ and $CD4^+$ gates for the lymphocyte panel or $CD3^-$ $CD19^-$ gate for the myeloid panel. We then randomly sampled 3000 cells from the final gate per animal for our analysis (or all available cells, if less than 3000) and used a t-distributed stochastic neighbor embedding (t-SNE) Barnes-hut algorithm to reduce the dimensionality of the data-set for visualization (57). In order to cluster the data appropriately, a network graph was created using k-nearest neighbors (k = 60), and a clustering solution was solved for by maximizing the modularity of the graph in a method adopted by Levine et.al. (58). All visualizations of clustering solutions through the use of t-SNE heatmaps, conventional heatmaps, and high-dimensional flow data were generated with the use of ExCYT, a MATLAB-based graphical user interface (GUI) for high-dimensional cytometry analysis (59).

Immunohistochemistry (IHC)

Tissues were dissected and fixed in 10% formalin solution prior to paraffin embedding, sectioning, and preparing slides. H&E staining was performed on each specimen for tumor pathologic analysis. Immunohistochemistry was performed on Plus Slides for mouse CD8α and FoxP3 expression by the Oncology Tissue Services Core at Johns Hopkins University. Images were acquired on a Nikon Eclipse E600 and imaged on a Nikon DS-Fi2 camera at 10× magnification.

Statistical Analysis

Survival data were plotted using Kaplan-Meier curves and statistical significance was determined using log-rank test. For tumor growth data, statistical significance was determined using a two-way ANOVA with Tukey's multiple comparisons test. Bar graphs represent mean ± SD (n = 3–5 mice per group). Dot plots show one mouse per dot, and each bar represents mean ± SEM. Significance was determined by a one-way ANOVA with Tukey's multiple comparisons test. Statistically significant p values are abbreviated as follows: *$p < 0.05$, **$p < 0.01$, ***$p < 0.001$, ****$p < 0.0001$. All statistical analyses were performed using GraphPad Prism v7.00.

RESULTS

A CD40 agonist improves antitumor efficacy of anti–PD-1 therapy

In the *neu*-N model of breast cancer, mice constitutively express rat neu and are tolerized against the neu antigen (44). We previously reported that a vaccine consisting of 3T3 cells expressing HER-2/neu and GM-CSF (3T3neuGM) induced $CD8^+$ neu-specific T cell responses against the immunodominant epitope $RNEU_{420–429}$ and resulted in eradication of

neu-expressing tumors (NT2.5 cells) in about 20% of HER-2/neu transgenic (*neu*-N) mice (41,43). Tumors develop with low baseline immune infiltration with a predominance of macrophages and G-MDSCs, some Tregs, and few effector T cells (Supplementary Fig. S1). We utilized this model to assess the effects of drug combinations on antitumor immune responses. Tumor-bearing mice were treated with either 3T3neuGM + PD-1 mAb alone or in combination with CD40 mAb, or isotype control mAbs, and monitored for tumor clearance and survival (Fig. 1A). Mice treated with 3T3neuGM + PD-1 mAb + CD40 mAb (triple therapy) had delayed tumor progression and increased median survival relative to isotype controls ($p<0.0001$), CD40 mAb ($p<0.0001$) or 3T3neuGM + PD-1 mAb treatment alone ($p<0.05$, Fig. 1B, C).

Although delayed tumor growth was promising, the majority of mice in all groups eventually succumbed to tumors, leaving room for improvement. We previously reported development of $CD8^+$ T cell receptor (TCR) transgenic mice that recognize the immunodominant epitope $RNEU_{420–429}$ (41). We showed that the 3T3neuGM vaccine given with adoptive transfer of 6×10^6 TCR transgenic T cells into tumor-bearing *neu*-N mice leads to tumor clearance in the majority of animals, whereas the 3T3neuGM vaccine given with 2×10^6 T cells only eradicates tumors in 20% of mice (42). We tested whether triple therapy improved the effect of 3T3neuGM + PD-1 if a sub-optimal number of TCR transgenic T cells (2×10^6) were introduced. Only mice receiving the TCR transgenic T cells in combination with 3T3neuGM + PD1 + CD40 resulted in 100% tumor clearance. In contrast, only 30% of mice treated with 3T3neuGM + PD1 were able to clear tumors, and none of the mice receiving isotype or CD40 mAbs alone had long-term survival (Fig. 1D, E). The 3T3neuGM vaccine was necessary for the combination antibody treatment to be effective, as treatment with PD1 + CD40 mAb alone failed to clear tumor in this model (Supplementary Fig. S2A, B).

Triple therapy was next evaluated in a metastatic PDAC model in which the mouse tumor PANC02 cells were introduced into wild-type recipients via intrasplenic injection followed by hemisplenectomy to allow liver metastases to develop (Fig. 1F, ref. 47,60). Mice treated with isotype control mAbs succumbed to metastatic disease at 37–62 days (median survival 60 days). A PANC02 vaccine (PANC02vac, irradiated PANC02 cells mixed with a GM-CSF secreting cell line) + anti–PD-1 treatment showed some efficacy, although 50% of mice developed fatal liver metastases (median survival 107.5 days). CD40 agonist mAb was active against PANC02 liver metastases, with 70% long-term survival following a single dose (survival >120 days), and mice treated with PANC02vac + PD1 + CD40 had 100% survival at 120 days. To evaluate primary tumor progression in addition to metastatic survival in PDAC, we utilized a third model in which PANC02 cells were introduced subcutaneously. Similarly, only mice receiving triple therapy remained 100% tumor-free over the course of the study. CD40 mAb and PANC02vac+PD1 alone were only able to clear tumor in 30% of mice (Fig. 1G).

Triple therapy enhances T-cell infiltration and function in murine solid tumors

A hallmark of most non-immunogenic cancers is lack of TIL and/or failure to mount a robust antitumor T cell response. To determine whether triple therapy induces effective T cell responses in mammary tumors, we treated tumor bearing *neu*-N mice with established

(>5×5 mm) NT2.5 tumors with either CD40 mAb alone, 3T3neuGM + PD1, 3T3neuGM + PD1 + CD40, or isotype mAb, with 6×10^6 TCR transgenic T cells, and harvested tumors and TDLN at Day 6 post-vaccine for analysis of T-cell proliferation, infiltration and function. Flow cytometry analysis of the TDLN revealed that adoptively transferred neu-specific T cells (Thy1.2$^+$) were significantly increased with triple therapy compared to all other groups, with a 25-fold expansion compared to isotype mAb, a 2.4-fold expansion compared to CD40 mAb treatment, and a nearly 100-fold expansion compared to 3T3neuGM + PD1 treatment at Day 6 post-vaccine (Supplementary Fig. S2C, ($p<0.0001$, $p<0.01$ and $p<0.0001$, respectively). Increased absolute T cell number was associated with increased Ki67 expression (Supplementary Fig. S2D, $p<0.001$) and CFSE dilution (Supplementary Fig. S2E, $p<0.0001$). CD40 antibody administration significantly impacted the capacity of 3T3neuGM + PD1 therapy to expand total T cell numbers, and could partially account for increased tumor clearance and survival observed. Flow cytometry analysis of tumors revealed that neu-specific T cells were significantly increased in 3T3neuGM + PD1 + CD40 treated mice compared to all other groups ($p<0.01$), with no change in endogenous CD8$^+$ T cells (Thy1.2$^-$), CD4$^+$ Th cells, or Tregs, relative to isotype mAb–treated mice (Fig. 2A, Supplementary Fig. S2F). Significantly increased tumor CD8$^+$ T cell/Treg ratio, a measure of immune robustness, was noted with triple therapy compared to all other groups (Fig. 2B, $p<0.001$). In contrast, there were twice as many Tregs in the tumors of 3T3neuGM + PD1 treated mice compared to mice receiving triple therapy (Supplementary Fig. S2F, $p<0.05$), and overall the CD8$^+$ T cell/Treg ratio was similar to isotype mAb treated mice (Fig. 2B). This pattern of T cell infiltration was observed on immunohistochemistry (IHC) analysis (Supplementary Fig. S3). T cell activation was measured by the number of IFNγ-, Granzyme B-, and TNFα-secreting CD8$^+$ TIL per mg tumor following 24 hours of *in vitro* stimulation with *neu*-peptide–pulsed T2D^q APCs. Granzyme B- and IFNγ-expressing cells were increased in TIL following both 3T3neuGM + PD1 and triple therapy, with triple therapy resulting in significantly more cells compared to CD40 mAb alone (Fig. 2C). Only mice receiving triple therapy had increased TNFα$^+$ T cells, as well as dual and triple cytokine–secreting polyfunctional T cells, compared to all other treatment groups (Figure 2C). In the TDLN, CD40 and 3T3neuGM + PD1 treatment alone led to increased cytokine-expressing CD8$^+$ T cells, with a further increase observed with triple therapy, including Granzyme B$^+$, TNFα$^+$, and polyfunctional T effector cells (Fig. 2D, $p<0.05$).

In the PANC02 hemispleen model we measured T-cell infiltration into liver metastases after 3 weeks of treatment (Fig. 2E). Similarly, endogenous CD8$^+$ T cells were increased in mice receiving triple therapy, along with PANC02vac + PD1 treated mice. CD4$^+$ Th and Treg cells were increased with PANC02vac + PD1 and PANC02vac + PD1 + CD40 treatment compared to isotype and CD40 mAb treatment ($p<0.001$ and $p<0.01$ for Th and Treg cells, respectively). Overall, only CD40 mAb treatment led to improvement in CD8$^+$ T cell/Treg ratio (CD8$^+$ T cell/Treg ratio of 10.8 vs. 21.6 for isotype mAb and CD40 mAb, respectively, $p<0.01$, from data shown in Fig. 2E), but liver TIL had increased cytokine-secreting CD8$^+$ T cells following stimulation with CD3/CD28 activating beads in all treatment groups (Fig. 2F).

Given the efficacy of triple therapy readily observed in the sc PDAC model (Fig. 1G) with endogenous T cells alone, we depleted CD4$^+$ or CD8$^+$ T cells in PANC02 sc tumor bearing

mice during treatment, then monitored tumor progression and survival. Depletion of either $CD4^+$ or $CD8^+$ T cells reduced tumor clearance rate of triple therapy to 20% (Fig. 2G, Supplementary Fig. S4A). $CD8^+$ T cell depletion completely abolished efficacy of CD40 mAb and PANC02vac + PD1 treatment, with 0% tumor clearance compared to 30% in undepleted mice (Supplementary Fig. S4B, C). $CD4^+$ T cell depletion did not impact tumor clearance in the CD40 mAb alone group, with 50% of mice remaining tumor-free, whereas tumor clearance rate was reduced from 30% to 10% in the PANC02vac + PD1 treatment group with $CD4^+$ T cell depletion (Supplementary Fig. S4B, C). Isotype mAb treated mice all developed tumors, regardless of T cell depletion status (Supplementary Fig. S4D). In the *neu*-N model, we can conclude that $CD8^+$ T cells are required for tumor clearance, as long-term survival could only be achieved with triple therapy when *neu*-specific $CD8^+$ T cells were introduced. However, efficacy of triple therapy in the *neu*-N model is completely independent of $CD4^+$ T cells, with 100% tumor clearance even in their absence (Supplementary Fig. S4E).

Triple therapy promotes the development of functional T cell memory

We evaluated the contribution of memory T cells to long-term survival with triple therapy. TIL and TDLN isolated from n*eu*-N mice at Day 15 post-treatment were analyzed by flow cytometry for abundance of naïve, central memory (T_{CM}) and effector memory (T_{EM}) $CD4^+$ and $CD8^+$ T cells (Fig. 3A–D). As anticipated, few naïve and T_{CM} cells were among the TIL in all cohorts (Fig. 3A, B). However, $CD4^+$ T_{EM} cells were increased with triple therapy compared to isotype and CD40 mAb therapy (Fig. 3A, $p<0.05$), whereas $CD8^+$ T_{EM} cells were increased in tumors of mice treated with CD40 mAb alone (Fig. 3B, $p<0.01$). To test durability of T cell responses, tumor-free mice were rechallenged with NT2.5 tumors in the contralateral mammary fat pad. Mice that initially received triple therapy showed some resistance to tumor rechallenge compared to previously untreated (naïve) tumor-challenged *neu*-N mice, with a median survival of 48 days post-rechallenge vs. 32 days for naïve mice (Fig. 3E, F). Similar results were observed in the PANC02 subcutaneous model, but all mice that received prior triple therapy remained tumor-free following rechallenge with PANC02 cells on the contralateral lower limb (Fig. 3G, H). This indicates development of a persistent functional memory T cell population that prevents formation of new tumors.

Triple therapy converts TME T cells from naïve T cells and Tregs to activated CTLs

To conduct a more detailed and unbiased analysis of immune populations in the tumors of treated mice, we applied high-dimensional clustering and t-SNE visualization to multicolor flow cytometry data. We collected TIL from *neu*-N mice treated with 3T3neuGM + PD1 with and without CD40 mAb and stained them with a panel of T cell marker mAbs. Live $CD4^+$ and $CD8^+$ T cells were identified and a fixed number of T cells from each tumor were clustered based on mean fluorescence intensity (MFI) of each parameter, including FoxP3, PD-1, CTLA4, and Tim3 (Fig. 4A, Supplementary Fig. S5A–C). Fourteen unique clusters were identified, with 6 key clusters labeled on the t-SNE plots and phenotypically characterized on high dimensional flow plots (Fig. 4A, B). We observed a significant shift in the lymphoid composition of the tumors in each treatment group (Fig. 4A, B). Isotype mAb treated mice had predominantly T cells that cluster into a $CD4^+$ Th and Treg phenotype (Clusters 10 and 6, respectively), as well as naïve $CD8^+$ endogenous T cells (Cluster 1). In

contrast, CD40 mAb treated mice had relatively decreased Th and Treg cells and a larger proportion of Thy1.2$^+$ CTLs with high CTLA4 expression (Cluster 4). 3T3neuGM + PD1–treated tumors demonstrated a significant frequency of Thy1.2$^+$ CTLs (Clusters 4, 5, and 14). Cluster 5, which had the highest PD-1 and Tim3 coexpression, was the most highly represented in this treatment group. Triple therapy treated mice had the greatest frequency of activated CD8$^+$ CTLs overall (Clusters 4 and 14), which moderately expressed PD-1 and CD40L, but were largely Tim3 and Gal3 negative. These populations correlated with response to treatment, and likely indicate T-cell activation and not exhaustion.

To confirm these CD8$^+$ CTLs represented activation rather than exhaustion, we explored dynamics of the cell populations identified by Clusters 4, 5 and 14. Specifically, expression of PD-1 and Tim3 in CD8$^+$ TIL was assessed at Days 4, 6, and 8 post-treatment (Fig. 5A). We expected Tim3 expression to increase over time if cells were becoming exhausted following gain of PD-1 expression. In all treatment groups of mice, Thy1.2$^+$ TIL were mostly PD-1$^+$ with minimal expression of Tim3 (i.e. Clusters 4 and 14). There was a transient increase in Tim3 expression in a small subset of PD-1$^+$ Thy1.2$^+$ T cells at Day 6, analogous to the PD-1$^+$ Tim3$^+$ population in Cluster 5. This population is somewhat diminished by Day 8, and is replaced by PD-1$^+$ Tim3$^-$ CTLs. Thy1.2$^-$ CD8$^+$ T cells had increased PD-1 expression at Day 6 in mice treated with triple therapy (Fig. 5B, $p<0.01$), andoverall the proportion of Thy1.2$^-$ CD8$^+$ T cells lacking PD-1 and Tim3 expression was reduced in mice treated with triple therapy relative to isotype or CD40 mAb therapy ($p<0.01$ and $p<0.05$, respectively). By Day 8, Thy1.2$^-$ T cells continued to gain PD-1 expression, a marker of activated CTLs, while losing Tim3 expression. This PD-1$^+$ population was highest in mice receiving triple therapy, indicating that combination treatment improves activation of endogenous CD8$^+$ T cells as well as TCR transgenic T cells.

Triple therapy alters the myeloid component of the TME

We tested whether increased T-cell activation and infiltration observed in mice receiving triple therapy was associated with changes in myeloid cell phenotype and/or function. We performed a similar t-SNE clustering analysis on the myeloid population (CD3$^-$ CD19$^-$) in tumors from treated *neu*-N mice (Fig. 6A, Supplementary Fig. S6A–C). The most notable difference observed was a significant increase in CD8$^+$ CD11c$^+$ DCs with triple therapy (Clusters 4 and 7, Fig. 6A, B), which highly expressed MHCII and CD86 and represent licensed APCs. Mice treated with 3T3neuGM + PD1 also had an increase in macrophages (cells expressing CD11b and F4/80) (Clusters 8 and 10) as well as a DC population, but it was a CD8$^-$ CD11c$^+$ phenotype, with low MHCII and CD86 expression (Cluster 5). G-MDSCs were increased with CD40 mAb treatment compared to isotype mAb and triple therapy (Cluster 12). A similar pattern was observed in Cluster 2, which contained a population of monocytic cells with dim Ly6C expression. Isotype mAb treated tumors contained predominantly non-myeloid cells (i.e. negative expression of all myeloid markers in the panel), and most likely represent contaminating tumor cells (Cluster 3).

Changes in the myeloid lineage shown by clustering analysis led us to further investigate infiltration and function of these cell populations. We performed additional characterization of TIL and TDLN cells by flow cytometry to look at expression of myeloid maturation

markers. Here we observed a significant decrease in G-MDSCs per mg of tumor in treated *neu*-N mice, whereas monocytic MDSC (M-MDSC) abundance was relatively unchanged (Fig. 7A). As with Clusters 8 and 10, $CD11b^+$ $F4/80^+$ macrophages were increased with treatment, particularly CD40 mAb and triple therapy (Fig. 7B). $CD8^+$ $CD11c^+$ $MHCII^+$ DCs (analogous to Clusters 4 and 7) were significantly increased with triple therapy relative to isotype and CD40 mAb alone, and increased with 3T3neuGM + PD1 only relative to isotype mAb (Fig. 7C). However, immature M-MDSCs and mature macrophages in tumors of mice treated with CD40 mAb and triple therapy had significantly decreased expression of arginase 1 (Arg1), an enzyme that contributes to immunosuppressive function (Fig. 7D). In addition, DCs assessed in the TDLN of CD40 mAb and triple therapy treated mice had significantly higher expression of the costimulatory molecules CD80 and CD86 (Fig. 7E), and a greater abundance of $CD103^+$ DCs (Fig. 7F). $CD103^+$ DCs are Batf3-dependent cross-presenting DCs thought to play a critical role in tumor antigen presentation (61,62). There was evidence of M1 macrophage polarization occurring in the TDLN with CD40 mAb and triple therapy, demonstrated by increased CD80 and CD86 expression (Fig. 7G, ref. (63). Frequency of $CD80^+$ macrophages was further increased with triple therapy compared to CD40 mAb alone. Finally, CD40 mAb and triple therapy led to a greater abundance of $CD169^+$ (Siglec1) macrophages in the TDLN, which are thought to serve as LN-resident APCs that activate tumor antigen-specific CTLs (Fig. 7H, (63).

Based on these data, triple therapy enhances maturation of multiple myeloid populations in the LN and TME. Distinct patterns were noted in expression of PD-L1 and MHCII in myeloid cell types. In the *neu*-N model, treatment with 3T3neuGM + PD1 + CD40 led to increased MHCII expression in conventional/classical non-plasmacytoid DCs and M-MDSCs (Supplementary Fig. S7A, B). M-MDSCs and G-MDSCs also gained expression of PD-L1, a ligand of PD-1 upregulated in response to IFNγ signaling (Supplementary Fig. S7B, C). There was a significant increase in coexpression of MHCII and PD-L1 in $CD11b^+$ $F4/80^+$ macrophages (Supplementary Fig. S7D). Similar patterns in myeloid cells were observed infiltrating PANC02 liver metastases (Supplementary Fig. S7E–H), although coexpression of MHCII and PD-L1 was more predominant in cDCs and $CD11b^+$ $F4/80^+$ macrophages in mice receiving triple therapy.

DISCUSSION

Development of I-O mAbs has revolutionized cancer therapy and reinvigorated the cancer immunology and immunotherapy field. However, most cancer types fail to respond to current single agent and combination I-O mAbs because of diversity among and within different tumors. New strategies that account for biologic differences are needed to convert immune resistant tumors into immunologically-primed tumors that can respond to ICIs. Our data show that naturally non-immunogenic tumors can be reprogrammed by combining a T cell–inducing vaccine with a costimulatory molecule agonist and an ICI to elicit antitumor immunity.

We found that optimal T cell activation required triple therapy with a T cell–inducing vaccine in combination with the DC maturing CD40 agonist and anti–PD-1. Coinciding with increased costimulatory molecule expression and MHCII expression on LN DCs, triple

therapy promoted trafficking and/or DC maturation in mammary tumor TME, with greater than a 30-fold increase relative to isotype mAb treated mice. The critical role of DCs in CD40 agonist combination therapy has been reported (32,64). These findings, together with observations that triple therapy is dependent on larger numbers of infiltrating $CD8^+$ T cells and less on $CD4^+$ T cells, supported by T cell depletion studies, suggests that mature DCs may directly prime CTLs in the TME. This possibility is supported by our prior observation of infiltrating lymphoid aggregates containing mature DCs in PDAC patients treated with a similar vaccine (65).

In addition to the role of maturing DCs for enhanced T-cell activation in the TDLN and the tumor, CD40 agonist activity alters infiltration and function of immunosuppressive cells in the TME. Triple therapy led to decreased tumor-infiltrating G-MDSCs and Tregs to further promote an active CTL response. Although there was expansion of $MHCII^{hi}$ $CD86^{hi}$ $CD11b^+$ $F4/80^+$ macrophages in the TME, expression of arginase 1 in macrophages and immature M-MDSCs was decreased, supporting our findings that CD40 agonist disarms functionality of multiple suppressor cell populations. Studies have reported macrophage-dependent tumor regression (66), particularly in PDAC, in which CD40-activated macrophages deplete the stromal cells within the TME (25). We showed that CD40 agonist activity matures multiple monocyte and DC populations to attract activated $CD8^+$ T cells. We observed increased PD-L1 expression on G-MDSCs, M-MDSCs, and macrophages, likely another indication of myeloid maturation occurring in these previously immunosuppressive cells. With a PD-1 antagonist as part of this treatment regimen, it is unlikely that these cells are able to exert a suppressive function through PD-L1.

These studies suggest that triple therapy efficacy may occur via different mechanisms in PDAC and breast tumor models. This may be due to the tumor type itself or the site of tumor development or metastasis. Understanding the role of monocyte and T cell populations between tumor types and sites may inform the optimal combination immunotherapies for patients. Both models showed increased Th1 cytokine production in the TME that corresponded with improved survival. Yet the $CD8^+$ T cell/Treg ratio, significantly increased with triple therapy in *neu*-N mice, was not elevated in the PDAC model. The increased rate of tumor clearance between triple therapy and PANC02vac + PD1 in the PDAC model (100% vs. 30–50%) could not be accounted for by differences in T cell infiltration alone. *In vivo* T-cell depletion is useful to delineate the contributions of $CD4^+$ and $CD8^+$ T cell subsets in treatment efficacy. Both $CD4^+$ and $CD8^+$ T cells were required for tumor clearance with triple therapy in the subcutaneous PDAC model. CD40 agonists may act via a $CD4^+$ T cell–independent mechanism, and as anticipated, depletion of $CD4^+$ T cells did not impact survival of mice treated with CD40 mAb alone. There was a trend toward increased survival in absence of $CD4^+$ T cells, with 50% of mice achieving long-term tumor free survival, compared to 30% of un-depleted mice, similar to other reports involving therapeutic CD40 pathway stimulation (15,67). This could be due to the fact that Th cells and Tregs are being depleted simultaneously with anti-CD4, the latter of which may account for the trend towards improved survival. In the *neu*-N model, $CD8^+$ T cells were required for tumor clearance (triple therapy only results in long-term survival with adoptive T cell therapy of *neu*-specific $CD8^+$ T cells). Triple therapy efficacy was completely independent of $CD4^+$ T cells in this model, with 100% tumor clearance even in their absence. Thus, triple

therapy efficacy relies on $CD8^+$ T cells in both models, but the role of $CD4^+$ T cell help might be more important in the PDAC model, in which endogenous antigen-specific T cells need to be induced and therefore require APC and Th cell crosstalk.

In summary, T cell–inducing vaccines in combination with an agonist monocyte/DC maturing antibody and PD-1 antagonist mAb synergize to induce durable antitumor immunity. CD40 mAb improves T-cell activation in the TDLN but is not sufficient to promote tumor infiltration on its own. CD40 mAb and the combination of CD40 + PD-1 mAbs fail to substantially increase $CD8^+$ TIL. Therefore, vaccine administration is required to promote T cell infiltration into tumor tissue. Triple therapy with vaccine and dual agonist-antagonist mAbs potentially synergizes by means of the vaccine providing abundant tumor antigen and early APC maturation in the lymph node. This is followed by CD40-induced upregulation of costimulatory molecules and enhanced APC maturation in the lymph node, which promotes $CD8^+$ T cell activation, proliferation, and trafficking into the TME. These results provide a model for converting non-immunogenic tumors into immune responsive cancers.

Supplementary Material

Refer to Web version on PubMed Central for supplementary material.

Acknowledgements

HSM designed the study, designed and performed experiments, analyzed data, and wrote the manuscript. BP and JWS designed and performed experiments, analyzed data, and edited the manuscript. ERT, TMR and BC performed experiments and edited the manuscript. BS, KC, and SW performed experiments. VZW and TA designed experiments, analyzed data and edited the manuscript. EMJ designed the study, designed experiments, edited the manuscript, and supervised the study.

Funding: NIH R01CA184926, NIH P30CA006973 (Sidney Kimmel Comprehensive Cancer Center grant), NIH P50CA062924 (Gastrointestinal cancers Spore grant), Research supported by a Stand Up To Cancer Colorectal Cancer Dream Team Translational Research Grant (Grant Number: SU2C-AACR-DT14-14). Stand Up To Cancer is a division of the Entertainment Industry Foundation. Research grants are administered by the American Association for Cancer Research, the Scientific Partner of SU2C. Dr. Jaffee also acknowledges funding from the Broccoli Foundation, The Bloomberg~Kimmel Institute for Cancer Immunotherapy, and The Skip Viragh Center for Pancreas Cancer Clinical Research and Patient Care. Dr. Roussos Torres is funded through the MacMillan Pathway to Independence Fellowship as well as a training grant (5T32 CA009071-34). Dr. Robinson has salary support through the institutional hematology training grant (T32 HL 7525-33). Blake Scott is supported by the National Science Foundation Graduate Research Fellowship under Grant No. DGE-1232825. Any opinion, findings, and conclusions or recommendations expressed in this material are those of the authors(s) and do not necessarily reflect the views of the National Science Foundation.

Conflicts of Interest: Through a licensing agreement with JHU, Dr. Jaffee has the potential to receive royalties from Aduro for a human GVAX vaccine. Dr. Jaffee receives research funding from Aduro Biotech and Bristol Myer Squibb.

REFERENCES

1. Topalian SL, Hodi FS, Brahmer JR, Gettinger SN, Smith DC, McDermott DF, et al. Safety, Activity, and Immune Correlates of Anti–PD-1 Antibody in Cancer. N Engl J Med 2012;366:2443–54. [PubMed: 22658127]
2. Weber JS, P D'Angelo S, Minor D, Hodi FS, Gutzmer R, Neyns B, et al. Nivolumab versus chemotherapy in patients with advanced melanoma who progressed after anti-CTLA-4 treatment (CheckMate 037): a randomised, controlled, open-label, phase 3 trial. Lancet Oncology Elsevier Ltd; 2015;16:375–84. [PubMed: 25795410]

3. Robert C, Long GV, Brady B, Dutriaux C, Maio M, Mortier L, et al. Nivolumab in Previously Untreated Melanoma without BRAFMutation. N Engl J Med 2015;372:320–30. [PubMed: 25399552]

4. Larkin J, Chiarion-Sileni V, Gonzalez R, Grob JJ, Cowey CL, Lao CD, et al. Combined Nivolumab and Ipilimumab or Monotherapy in Untreated Melanoma. N Engl J Med 2015;373:23–34. [PubMed: 26027431]

5. Sharma P, Allison JP. The future of immune checkpoint therapy. Cancer Immunol Immunother 2015;348:56–61.

6. Mittal D, Gubin MM, Schreiber RD, Smyth MJ. New insights into cancer immunoediting and its three component phases—elimination, equilibrium and escape. Current Opinion in Immunology 2014;27:16–25. [PubMed: 24531241]

7. DuPage M, Mazumdar C, Schmidt LM, Cheung AF, Jacks T. Expression of tumour-specific antigens underlies cancer immunoediting. Nature Nature Publishing Group; 2012;482:405–9. [PubMed: 22318517]

8. Clark CE, Beatty GL, Vonderheide RH. Immunosurveillance of pancreatic adenocarcinoma: Insights from genetically engineered mouse models of cancer. Cancer Letters Elsevier Ireland Ltd; 2009;279:1–7. [PubMed: 19013709]

9. Clark CE, Hingorani SR, Mick R, Combs C, Tuveson DA, Vonderheide RH. Dynamics of the Immune Reaction to Pancreatic Cancer from Inception to Invasion. Cancer Research 2007;67:9518–27. [PubMed: 17909062]

10. Tassi E, Gavazzi F, Albarello L, Senyukov V, Longhi R, Dellabona P, et al. Carcinoembryonic Antigen-Specific but Not Antiviral CD4+ T Cell Immunity Is Impaired in Pancreatic Carcinoma Patients. The Journal of Immunology 2008;181:6595–603. [PubMed: 18941250]

11. Gabitass RF, Annels NE, Stocken DD, Pandha HA, Middleton GW. Elevated myeloid-derived suppressor cells in pancreatic, esophageal and gastric cancer are an independent prognostic factor and are associated with significant elevation of the Th2 cytokine interleukin-13. Cancer Immunol Immunother 2011;60:1419–30. [PubMed: 21644036]

12. Vonderheide RH, Bayne LJ. Inflammatory networks and immune surveillance of pancreatic carcinoma. Current Opinion in Immunology 2013;25:200–5. [PubMed: 23422836]

13. Fu J, Malm IJ, Kadayakkara DK, Levitsky H, Pardoll D, Kim YJ. Preclinical Evidence That PD1 Blockade Cooperates with Cancer Vaccine TEGVAX to Elicit Regression of Established Tumors. Cancer Research 2014;74:4042–52. [PubMed: 24812273]

14. Binder DC, Engels B, Arina A, Yu P, Slauch JM, Fu YX, et al. Antigen-Specific Bacterial Vaccine Combined with Anti-PD-L1 Rescues Dysfunctional Endogenous T Cells to Reject Long-Established Cancer. Cancer Immunology Research 2013;1:123–33. [PubMed: 24455752]

15. Cho H-I, Jung S-H, Sohn H-J, Celis E, Kim T-G. An optimized peptide vaccine strategy capable of inducing multivalent CD8 +T cell responses with potent antitumor effects. OncoImmunology 2015;4:e1043504–12. [PubMed: 26451316]

16. Ahrends T, Baba a N, Xiao Y, Yagita H, van Eenennaam H, Borst J. CD27 Agonism Plus PD-1 Blockade Recapitulates CD4+ T-cell Help in Therapeutic Anticancer Vaccination. Cancer Research 2016;76:2921–31. [PubMed: 27020860]

17. Hurwitz A, Yu T, Leach DR, Allison JP. CTLA-4 blockade synergizes with tumor-derived granulocyte– macrophage colony-stimulating factor for treatment of an experimental mammary carcinoma. Proc Natl Acad Sci 1998;95:10067–71. [PubMed: 9707601]

18. Wilgenhof S, Corthals J, Heirman C, van Baren N, Lucas S, Kvistborg P, et al. Phase II Study of Autologous Monocyte-Derived mRNA Electroporated Dendritic Cells (TriMixDC-MEL) Plus Ipilimumab in Patients With Pretreated Advanced Melanoma. Journal of Clinical Oncology 2016;34:1330–8. [PubMed: 26926680]

19. Madan RA, Mohebtash M, Arlen PM, Vergati M, Rauckhorst M, Steinberg SM, et al. Ipilimumab and a poxviral vaccine targeting prostate-specific antigen in metastatic castration-resistant prostate cancer: a phase 1 dose-escalation trial. The Lancet Oncology 2012;13:501–8. [PubMed: 22326924]

20. Ribas A, Comin-Anduix B, Chmielowski B, Jalil J, la Rocha de P, McCannel TA, et al. Dendritic cell vaccination combined with CTLA4 blockade in patients with metastatic melanoma. Clinical

Cancer Research American Association for Cancer Research; 2009;15:6267–76. [PubMed: 19789309]

21. Gibney GT, Kudchadkar RR, DeConti RC, Thebeau MS, Czupryn MP, Tetteh L, et al. Safety, Correlative Markers, and Clinical Results of Adjuvant Nivolumab in Combination with Vaccine in Resected High-Risk Metastatic Melanoma. Clinical Cancer Research 2015;21:712–20. [PubMed: 25524312]
22. Le DT, Lutz E, Uram JN, Sugar EA, Onners B, Solt S, et al. Evaluation of Ipilimumab in Combination With Allogeneic Pancreatic Tumor Cells Transfected With a GM-CSF Gene in Previously Treated Pancreatic Cancer. Journal of Immunotherapy 2013;36:382–9. [PubMed: 23924790]
23. Lutz ER, Wu AA, Bigelow E, Sharma R, Mo G, Soares K, et al. Immunotherapy Converts Nonimmunogenic Pancreatic Tumors into Immunogenic Foci of Immune Regulation. Cancer Immunology Research 2014;2:616–31. [PubMed: 24942756]
24. de Vos S, Forero-Torres A, Ansell SM, Kahl B, Cheson BD, Bartlett NL, et al. A phase II study of dacetuzumab (SGN-40) in patients with relapsed diffuse large B-cell lymphoma (DLBCL) and correlative analyses of patient-specific factors. Journal of Hematology Oncology 2014;7:1–9. [PubMed: 24387695]
25. Beatty GL, Gregory, Chiorean EG, Fishman MP, Saboury B, Teitelbaum UR, et al. CD40 Agonists Alter Tumor Stroma and Show Efficacy Against Pancreatic Carcinoma in Mice and Humans. Science 2011;331:1612–6. [PubMed: 21436454]
26. Rüter J, Antonia SJ, Burris HA, Huhn RD, Vonderheide RH. Immune modulation with weekly dosing of an agonist CD40 antibody in a phase I study of patients with advanced solid tumors. Cancer Biology & Therapy 2014;10:983–93.
27. Vonderheide RH, Flaherty KT, Khali M, Stumacher MS, Bajor DL, Hutnick NA, et al. Clinical Activity and Immune Modulation in Cancer Patients Treated With CP-870,893, a Novel CD40 Agonist Monoclonal Antibody. Journal of Clinical Oncology 2007;25:876–83. [PubMed: 17327609]
28. Curti BD, Kovacsovics-Bankowski M, Morris N, Walker E, Chisholm L, Floyd K, et al. OX40 Is a Potent Immune-Stimulating Target in Late-Stage Cancer Patients. Cancer Research 2013;73:7189–98. [PubMed: 24177180]
29. Segal NH, Logan TF, Hodi FS, McDermott D, Melero I, Hamid O, et al. Results from an Integrated Safety Analysis of Urelumab, an Agonist Anti-CD137 Monoclonal Antibody. Clinical Cancer Research 2017;23:1929–36. [PubMed: 27756788]
30. Grewal IS, Flavell RA. CD40 AND CD154 IN CELL-MEDIATED IMMUNITY. Annu Rev Immunol 1998;16:111–35. [PubMed: 9597126]
31. Vonderheide RH, Glennie MJ. Agonistic CD40 Antibodies and Cancer Therapy. Clinical Cancer Research 2013;19:1035–43. [PubMed: 23460534]
32. Sotomayor EM, Borrello I, Tubb E, Rattis F-M, Bien H, Lu Z, et al. Conversion of tumor-specific CD4+ T-cell tolerance to T-cell priming through in vivo ligation of CD40. Nat Med 1999;5:780–7. [PubMed: 10395323]
33. Beatty GL, Winograd R, Evans RA, Long KB, Luque SL, Lee JW, et al. Exclusion of T Cells From Pancreatic Carcinomas in Mice Is Regulated by Ly6Clow F4/80+ Extratumoral Macrophages. Gastroenterology Elsevier, Inc; 2015;149:201–10. [PubMed: 25888329]
34. Cho HI, Reyes-Vargas E, Delgado JC, Celis E. A Potent Vaccination Strategy That Circumvents Lymphodepletion for Effective Antitumor Adoptive T-cell Therapy. Cancer Research 2012;72:1986–95. [PubMed: 22367213]
35. Barrios K, Celis E. TriVax-HPV: an improved peptide-based therapeutic vaccination strategy against human papillomavirus-induced cancers. Cancer Immunol Immunother 2012;61:1307–17. [PubMed: 22527249]
36. Ahonen CL, Doxsee CL, McGurran SM, Riter TR, Wade WF, Barth RJ, et al. Combined TLR and CD40 Triggering Induces Potent CD8 +T Cell Expansion with Variable Dependence on Type I IFN. J Exp Med 2004;199:775–84. [PubMed: 15007094]

37. Hassan SB, Sørensen JF, Olsen BN, Pedersen AE. Anti-CD40-mediated cancer immunotherapy: an update of recent and ongoing clinical trials. Immunopharmacology and Immunotoxicology 2014;36:96–104. [PubMed: 24555495]

38. Luheshi NM, Coates-Ulrichsen J, Harper J, Mullins S, Sulikowski MG, Martin P, et al. Transformation of the tumour microenvironment by a CD40 agonist antibody correlates with improved responses to PD-L1 blockade in a mouse orthotopic pancreatic tumour model. Oncotarget 2016;7:18508–20. [PubMed: 26918344]

39. Winograd R, Byrne KT, Evans RA, Odorizzi PM, Meyer ARL, Bajor DL, et al. Induction of T-cell Immunity Overcomes Complete Resistance to PD-1 and CTLA-4 Blockade and Improves Survival in Pancreatic Carcinoma. Cancer Immunology Research 2015;3:399–411. [PubMed: 25678581]

40. Guy CT, Webster MA, Schaller M, Parsons TJ, Cardiff RD, Muller WJ. Expression of the neu protooncogene in the mammary epithelium of transgenic mice induces metastatic disease. Proc Natl Acad Sci 1992;89:10578–82. [PubMed: 1359541]

41. Ercolini AM, Ladle BH, Manning EA, Pfannenstiel LW, Armstrong TD, Machiels J-PH, et al. Recruitment of latent pools of high-avidity CD8 +T cells to the antitumor immune response. J Exp Med 2005;201:1591–602. [PubMed: 15883172]

42. Weiss VL, Lee TH, Song H, Kouo TS, Black CM, Sgouros G, et al. Trafficking of High Avidity HER-2/neu-Specific T Cells into HER-2/neu-Expressing Tumors after Depletion of Effector/ Memory-Like Regulatory T Cells. Kassiotis G, editor. PLoS ONE 2012;7:e31962–16. [PubMed: 22359647]

43. Machiels J-PH, Reilly RT, Emens LA, Ercolini AM, Lei RY, Okoye FI, et al. Cyclophosphamide, Doxorubicin, and Paclitaxel Enhance the Antitumor Immune Response of Granulocyte/ Macrophage-Colony Stimulating Factor- secreting Whole-Cell Vaccines in HER-2/. Cancer Research 2001;61:3689–97. [PubMed: 11325840]

44. Reilly RT, Gottlieb MBC, Ercolini AM, Machiels J-PH, Kane CE, Okoye FI, et al. HER-2/neu Is a Tumor Rejection Target in Tolerized HER-2/neu Transgenic Mice. Cancer Research 2000;60:3569. [PubMed: 10910070]

45. Kim PS, Armstrong TD, Song H, Wolpoe ME, Weiss V, Manning EA, et al. Antibody association with HER-2/neu–targeted vaccine enhances CD8+ T cell responses in mice through Fc-mediated activation of DCs. J Clin Invest 2008;118:1700–11. [PubMed: 18398507]

46. Ercolini AM, Machiels JPH, Chen YC, Slansky JE, Giedlen M, Reilly RT, et al. Identification and Characterization of the Immunodominant Rat HER-2/neu MHC Class I Epitope Presented by Spontaneous Mammary Tumors from HER-2/neu-Transgenic Mice. The Journal of Immunology 2003;170:4273–80. [PubMed: 12682262]

47. Soares KC, Foley K, Olino K, Leubner A, Mayo SC, Jain A, et al. A Preclinical Murine Model of Hepatic Metastases. JoVE 2014;:1–33.

48. Leao IC, Ganesan P, Armstrong TD, Jaffee EM. Effective Depletion of Regulatory T Cells Allows the Recruitment of Mesothelin-Specific CD8 +T Cells to the Antitumor Immune Response Against a Mesothelin-Expressing Mouse Pancreatic Adenocarcinoma. Clinical and Translational Science 2008;1:228–39. [PubMed: 20357913]

49. Levitsky HI, Hyam, Lazenby A, Hayashi R, Pardoll D. In Vivo Priming of Two Distinct Antitumor Effector Populations: Role of MHC Class I Expression. J Exp Med 1994;179:1215–24. [PubMed: 7908321]

50. Soares KC, Rucki AA, Wu AA, Olino K, Xiao Q, Chai Y, et al. PD-1/PD-L1 Blockade Together With Vaccine Therapy Facilitates Effector T-Cell Infiltration Into Pancreatic Tumors. Journal of Immunotherapy 2015;38:1–11. [PubMed: 25415283]

51. Twyman-Saint Victor C, Rech AJ, Maity A, Rengan R, Pauken KE, Stelekati E, et al. Radiation and dual checkpoint blockade activate non-redundant immune mechanisms in cancer. Nature 2015;520:373–7. [PubMed: 25754329]

52. Uddin MN, Zhang Y, Harton JA, MacNamara KC, Avram D. TNF- -Dependent Hematopoiesis following Bcl11b Deletion in T Cells Restricts Metastatic Melanoma. The Journal of Immunology 2014;192:1946–53. [PubMed: 24446520]

53. Kouo T, Huang L, Pucsek AB, Cao M, Solt S, Armstrong T, et al. Galectin-3 Shapes Antitumor Immune Responses by Suppressing CD8+ T Cells via LAG-3 and Inhibiting Expansion of

Plasmacytoid Dendritic Cells. Cancer Immunology Research 2015;3:412–23. [PubMed: 25691328]

54. Black CM, Armstrong TD, Jaffee EM. Apoptosis-Regulated Low-Avidity Cancer-Specific CD8+ T Cells Can Be Rescued to Eliminate HER2/neu-Expressing Tumors by Costimulatory Agonists in Tolerized Mice. Cancer Immunology Research 2014;2:307–19. [PubMed: 24764578]
55. Nomi T, Sho M, Akahori T, Hamada K, Kubo A, Kanehiro H, et al. Clinical Significance and Therapeutic Potential of the Programmed Death-1 Ligand/Programmed Death-1 Pathway in Human Pancreatic Cancer. Clinical Cancer Research 2007;13:2151–7. [PubMed: 17404099]
56. Sandin LC, Eriksson F, Ellmark P, Loskog AS, Tötterman TH, Mangsbo SM. Local CTLA4 blockade effectively restrains experimental pancreatic adenocarcinoma growth in vivo. OncoImmunology 2014;3:e27614–8. [PubMed: 24701377]
57. van der Maaten L Accelerating t-SNE using Tree-Based Algorithms. Journal of Machine Learning Research 2014;15:3221–45.
58. Levine JH, Simonds EF, Bendall SC, Davis KL, Amir E-AD, Tadmor MD, et al. Data-Driven Phenotypic Dissection of AML Reveals Progenitor-like Cells that Correlate with Prognosis. Cell 2015;162:184–97. [PubMed: 26095251]
59. Sidhom J-W, Theodros D, Murter B, Zarif J, Ganguly S, Pardoll D, et al. ExCYT: A Graphical User Interface for streamlining analysis of high-dimensional cytometry data
60. Zheng L, Foley K, Huang L, Leubner A, Mo G, Olino K, et al. Tyrosine 23 Phosphorylation-Dependent Cell-Surface Localization of Annexin A2 Is Required for Invasion and Metastases of Pancreatic Cancer. PLoS ONE 2011;6:1–16.
61. Broz ML, Binnewies M, Boldajipour B, Nelson AE, Pollack JL, Erle DJ, et al. Dissecting the Tumor Myeloid Compartment Reveals Rare Activating Antigen-Presenting Cells Critical for T Cell Immunity. Cancer Cell 2014;26:638–52. [PubMed: 25446897]
62. Roberts EW, Broz ML, Binnewies M, Headley MB, Nelson AE, Wolf DM, et al. Critical Role for CD103 + /CD141 + Dendritic Cells Bearing CCR7 for Tumor Antigen Trafficking and Priming of T Cell Immunity in Melanoma. Cancer Cell 2016;30:324–36. [PubMed: 27424807]
63. Chavez-Galan L, Olleros ML, Vesin D, Garcia I. Much More than M1 and M2 Macrophages, There are also CD169+ and TCR+ Macrophages. Front Immunol 2015;6:22–15. [PubMed: 25674091]
64. Dovedi SJ, Lipowska-Bhalla G, Beers SA, Cheadle EJ, Mu L, Glennie MJ, et al. Antitumor Efficacy of Radiation plus Immunotherapy Depends upon Dendritic Cell Activation of Effector CD8+ T Cells. Cancer Immunology Research 2016;4:621–30. [PubMed: 27241845]
65. Tsujikawa T, Kumar S, Borkar RN, Azimi V, Thibault G, Chang YH, et al. Quantitative Multiplex Immunohistochemistry Reveals Myeloid-Inflamed Tumor-Immune Complexity Associated with Poor Prognosis. Cell Reports 2017;19:203–17. [PubMed: 28380359]
66. Lum HD. In vivo CD40 ligation can induce T cell-independent antitumor effects that involve macrophages. Journal of Leukocyte Biology 2006;79:1181–92. [PubMed: 16565324]
67. Singh M, Vianden C, Cantwell MJ, Dai Z, Xiao Z, Sharma M, et al. Intratumoral CD40 activation and checkpoint blockade induces T cell-mediated eradication of melanoma in the brain. Nature Communications Springer US; 2017;1–10.

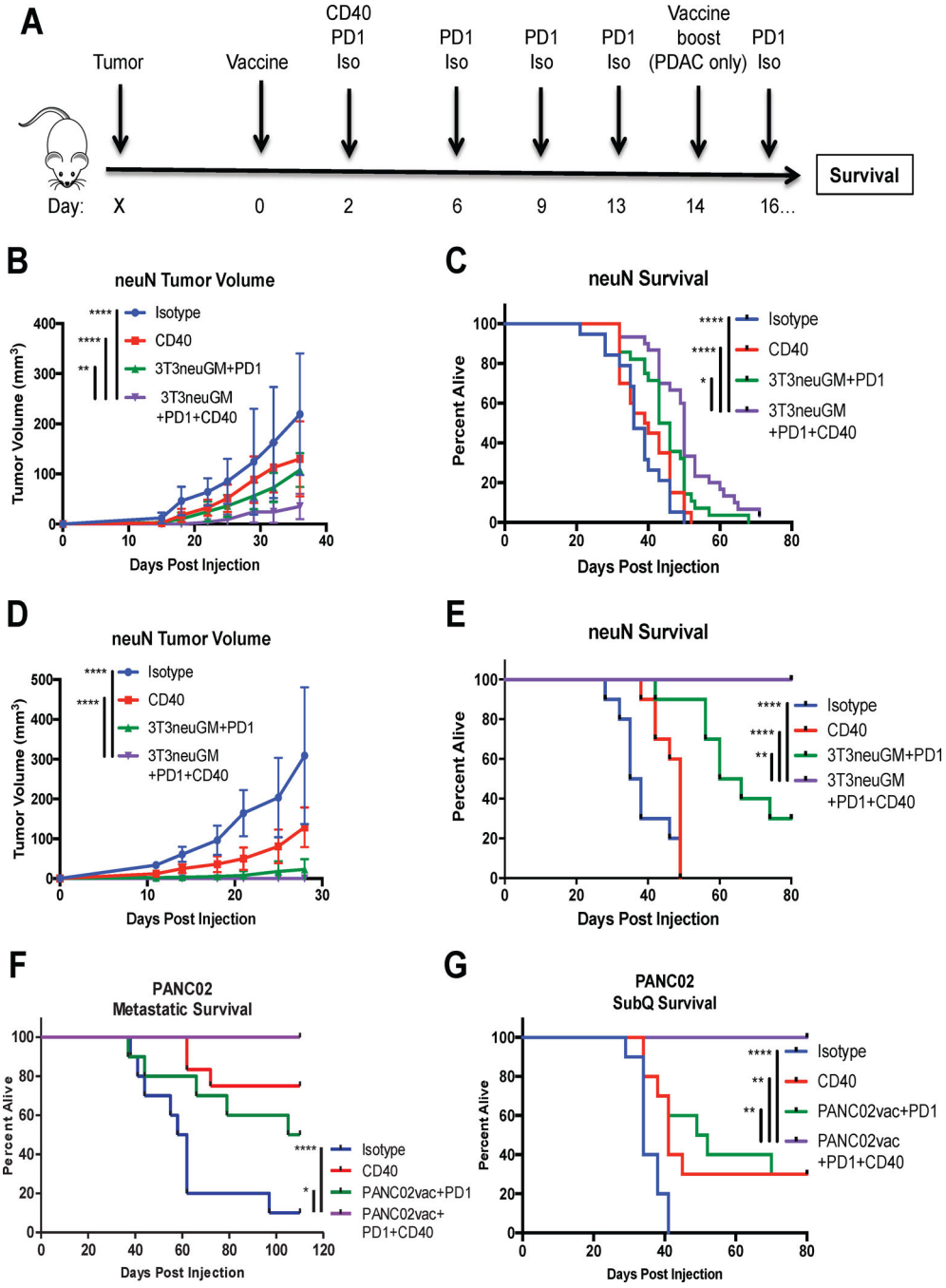

Figure 1. A CD40 agonist increases antitumor efficacy of vaccine + anti–PD-1 therapy.

A) Schematic. Mice are inoculated with tumor cells on day X, specified below, and treated with vaccine on Day 0, followed by anti–PD-1 and/or CD40 agonist mAb, or rat IgG isotype control, on Day 2. Anti–PD-1 therapy is continued twice weekly thereafter, until subcutaneous tumors reach >500 mm^3, or mice succumb to liver metastases (n = 10 mice per group). B) Tumor volume (n = 10 mice per group) and C) overall survival (n = 19–29 mice per group, pooled from 3 independent experiments) of *neu*-N mice given 5×10^4 NT2.5 cells in the mammary fat pad on Day X = −3 and treated as indicated. D) Tumor volume and E)

overall survival of *neu*-N mice given 5×10^4 NT2.5 cells in the mammary fat pad on Day X = −3, followed by 2×10^6 *neu*-specific $CD8^+$ T cells on Day 1, and treated as indicated. F) Overall survival of C57BL/6 mice given 2×10^6 PANC02 tumor cells via intrasplenic injection followed by hemisplenectomy on Day X = −15 and treated as indicated. G) Overall survival of C57BL/6 mice given 1×10^6 PANC02 tumor cells subcutaneously in the left lower limb on Day X = −15 and treated as indicated. *, $p<0.05$, **, $p<0.01$, ***, $p<0.001$, ****, $p<0.0001$.

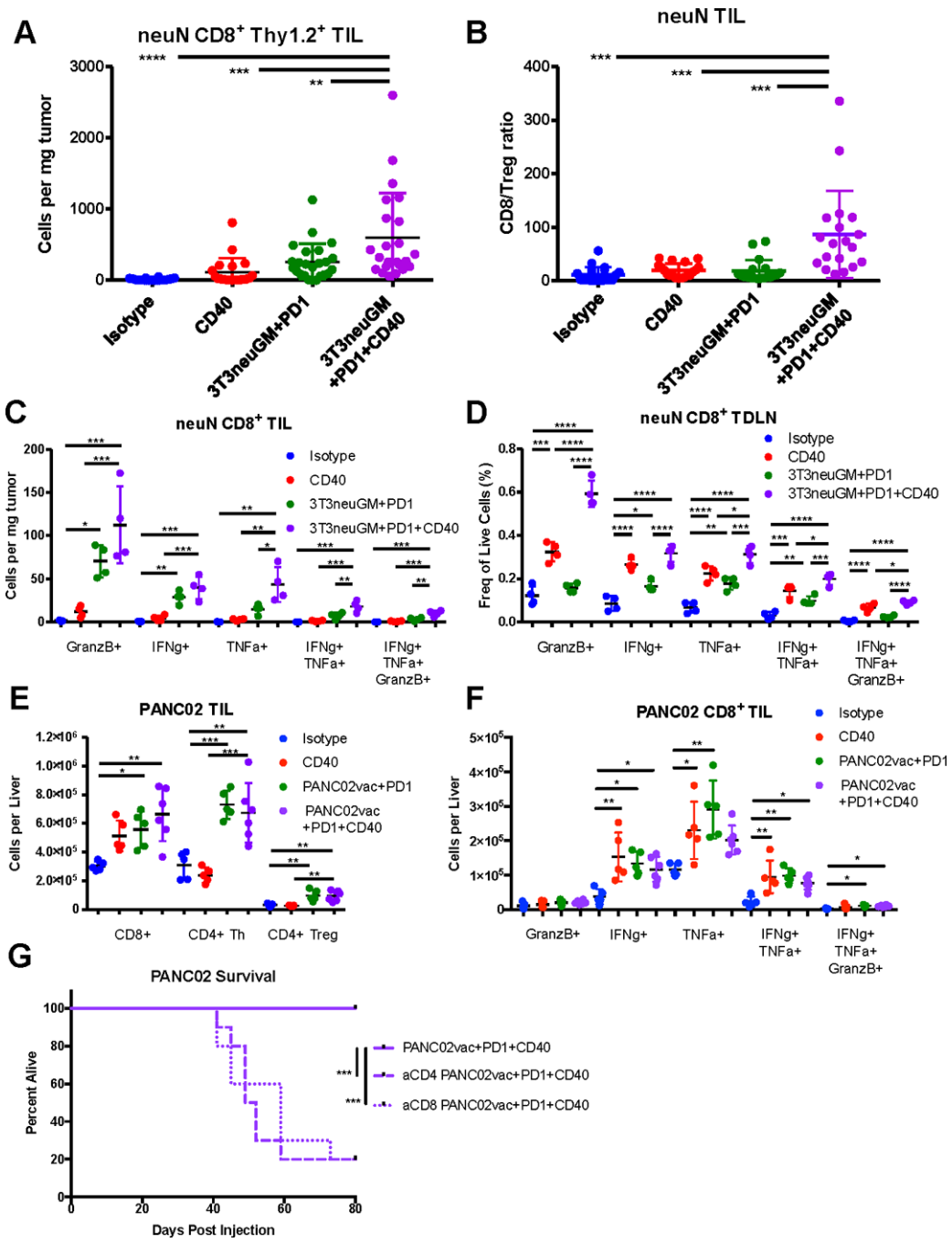

Figure 2. A CD40 agonist + vaccine + anti–PD-1 therapy induces cytotoxic T cell responses in mammary and pancreatic tumors.

A) Tumor infiltration of Thy1.2$^+$ CD8$^+$ T cells as measured by number of cells per mg tumor and B) CD8$^+$ T cell/Treg ratio as measured by number of CD8$^+$ T cells / number of CD4$^+$ FoxP3$^+$ T cells in tumors of *neu*-N mice (n = 20–24 mice per group, pooled from 6 independent experiments). Cytokine expression of CD8$^+$ T cells from *neu*-N mice following stimulation of C) TIL and D) TDLN cells with RNEU peptide-pulsed APCs (n = 3–4 mice per group). E) Liver infiltration of CD8$^+$, CD4$^+$ Th and CD4$^+$ Treg T cells as measured by number of cells per liver in PANC02 metastatic tumor-bearing mice. F) Cytokine expression

of $CD8^+$ T cells following stimulation of PANC02 liver TIL with CD3/CD28 activation beads. G) Overall survival of PANC02 subcutaneous tumor injected mice treated with depleting mAbs against CD8α, CD4, or isotype control. *, $p<0.05$, **, $p<0.01$, ***, $p<0.001$, ****, $p<0.0001$. TDLN=tumor draining lymph node; APCs=antigen presenting cells.

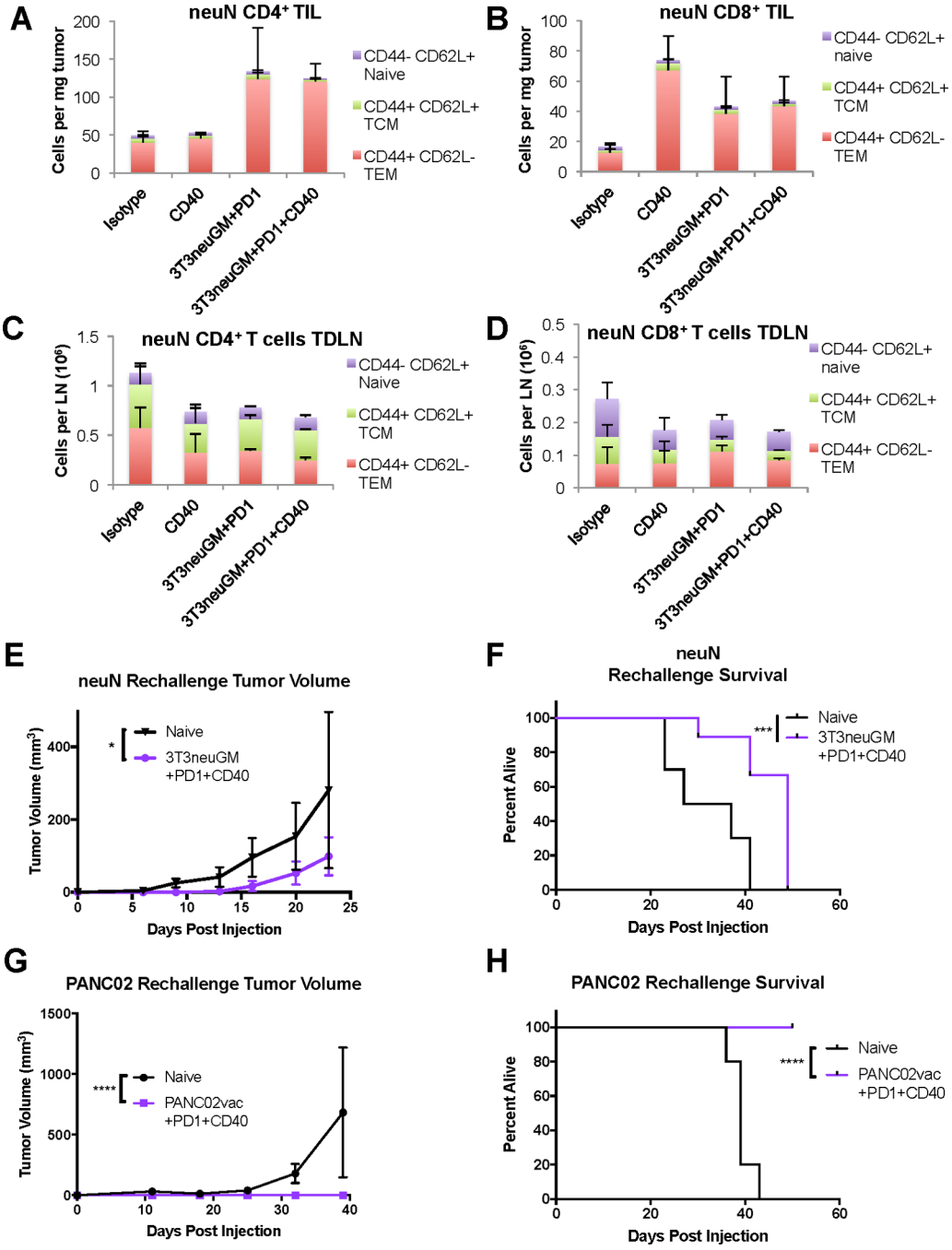

Figure 3. A CD40 agonist + vaccine + anti–PD-1 therapy induces T cell memory in tumors.

Tumor infiltration of A) $CD4^+$ and B) $CD8^+$ memory T cells as measured by number of cells per mg tumor, and C) $CD4^+$ and D) $CD8^+$ memory T cells in TDLN as measured by number of cells per LN on Day 14 in *neu*-N mice. E) Tumor volume and F) overall survival of triple therapy treated *neu*-N mice rechallenged with NT2.5 tumor cells on Day 28. *Neu*-N mice were inoculated with 1×10^6 tumor cells on Day −8 and treated with 3T3neuGM on Day 0 and 14, as well as 6×10^6 *neu*-specific T cells on Day 1. MAb therapy was administered as described until Day 28, at which point therapy was discontinued and tumor-free triple

therapy treated mice, or naïve controls, were rechallenged with 5×10^4 NT2.5 cells in the contralateral mammary fat pad. Graphs represent days post injection of rechallenge tumor. G) Tumor volume and H) overall survival of triple therapy treated mice rechallenged with PANC02 tumors cells in the contralateral lower limb (or naïve controls) on day 60. Graphs represent days post injection of rechallenge tumor **p<0.01, ****, p<0.0001.

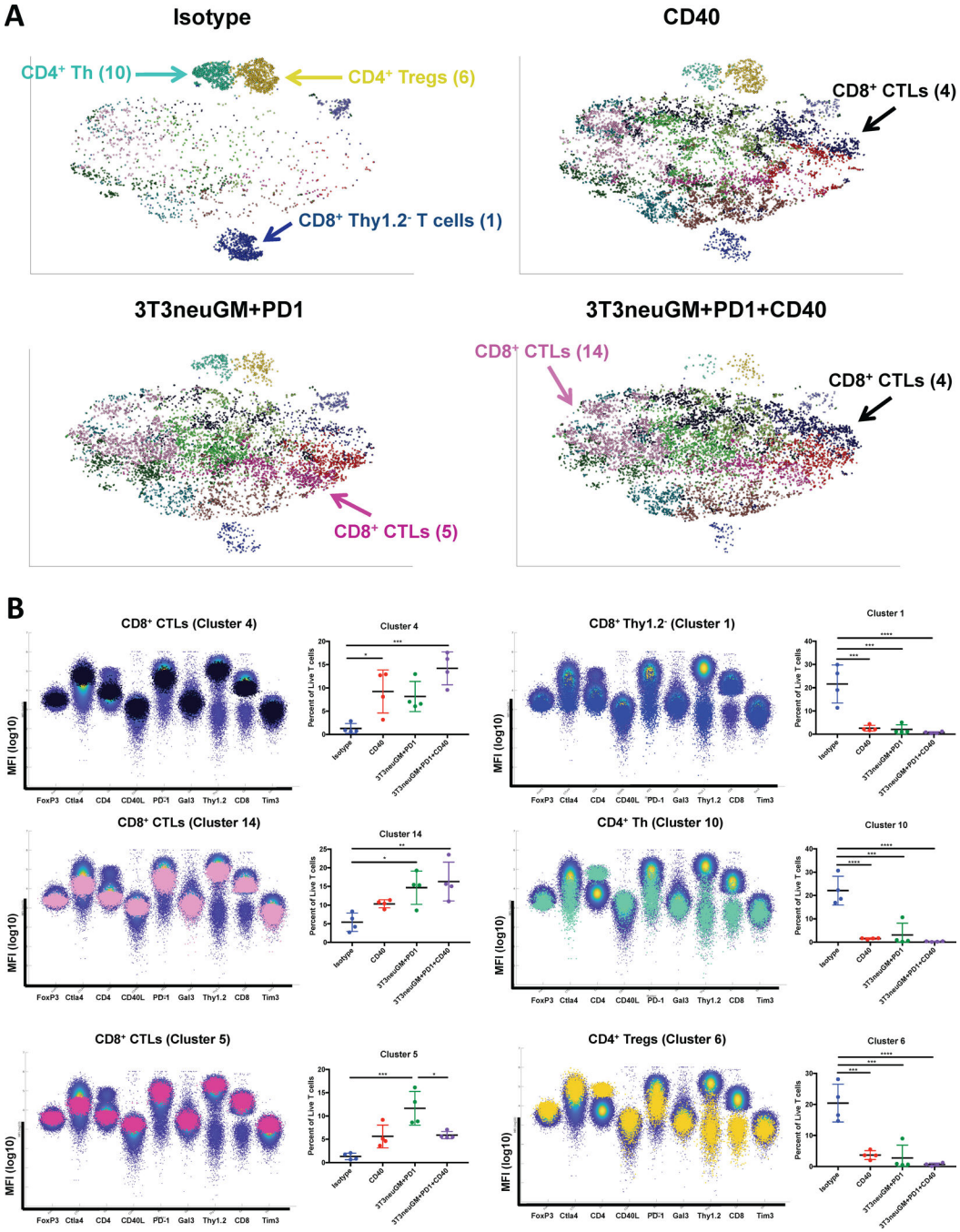

Figure 4. Lymphoid immune infiltrates shift from naïve T cells and Tregs to activated CTLs.

A) t-SNE plots of T cell clusters from tumors of *neu*-N mice, separated by treatment group. Samples were gated on Live/CD3$^+$/CD4$^+$CD8$^-$ or Live/CD3$^+$/CD8$^+$CD4$^-$ T cells (n = 4 mice per group). Key clusters are labeled with T cell phenotype and cluster number. B) High dimensional flow plots showing MFI of each T cell marker, with clusters highlighted according to cluster color and overlaid on total T cells. Dot plots show frequency of each cluster per treatment group, represented by percent of live T cells. *, p<0.05, **, p<0.01,

***, p<0.001, ****, p<0.0001. t-SNE = t-distributed stochastic neighbor embedding. MFI = mean fluorescence intensity.

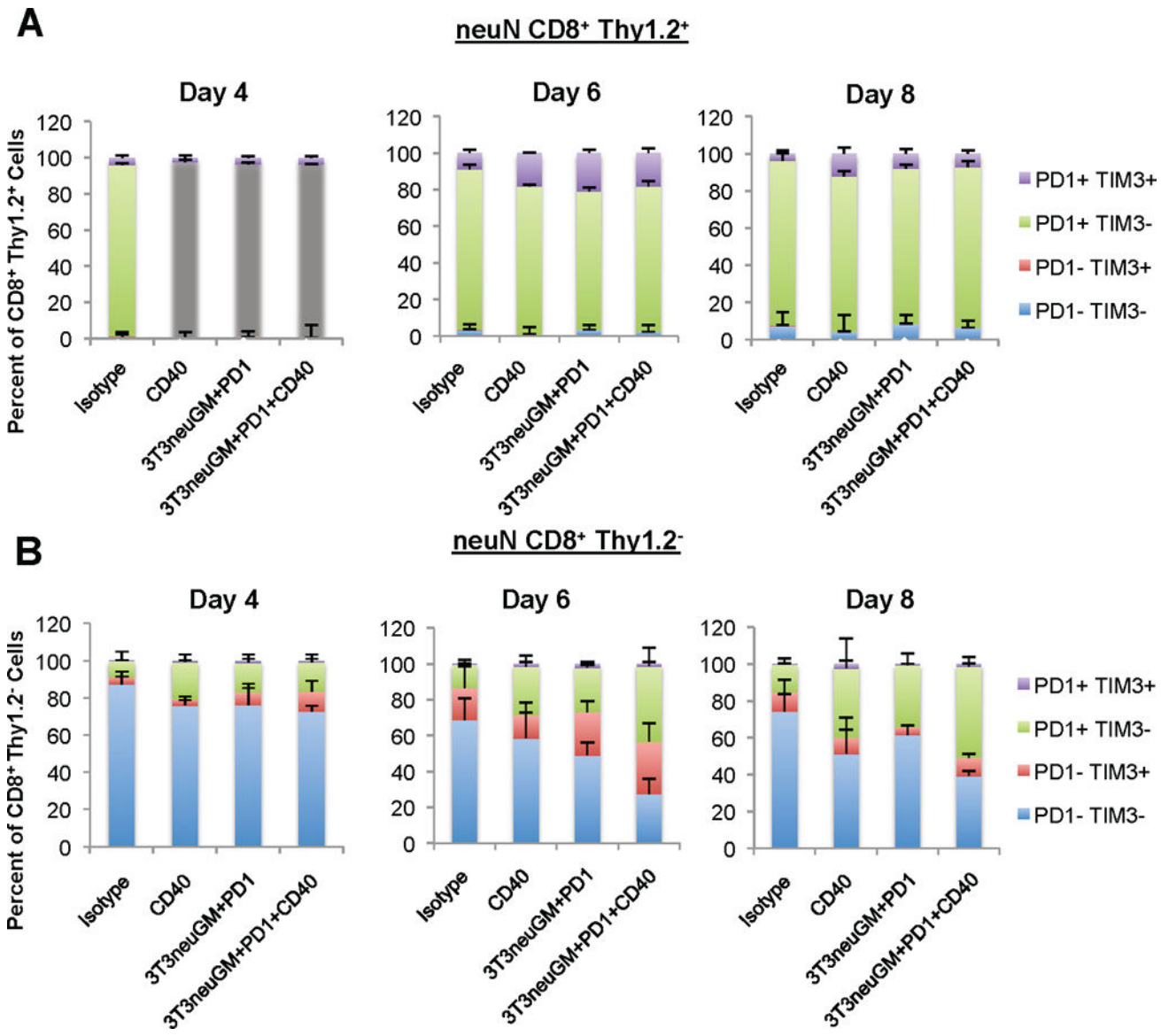

Figure 5. Markers of T-cell activation are increased with triple therapy.

PD-1 and Tim3 expression in A) Thy1.2^{+} CD8^{+} and B) Thy1.2^{-} CD8^{+} T cells on Day 4, 6 and 8 from tumors of treated *neu*-N mice, represented as frequency of parent population (Thy1.2^{+} CD8^{+} T cells or Thy1.2^{-} CD8^{+} T cells, respectively).

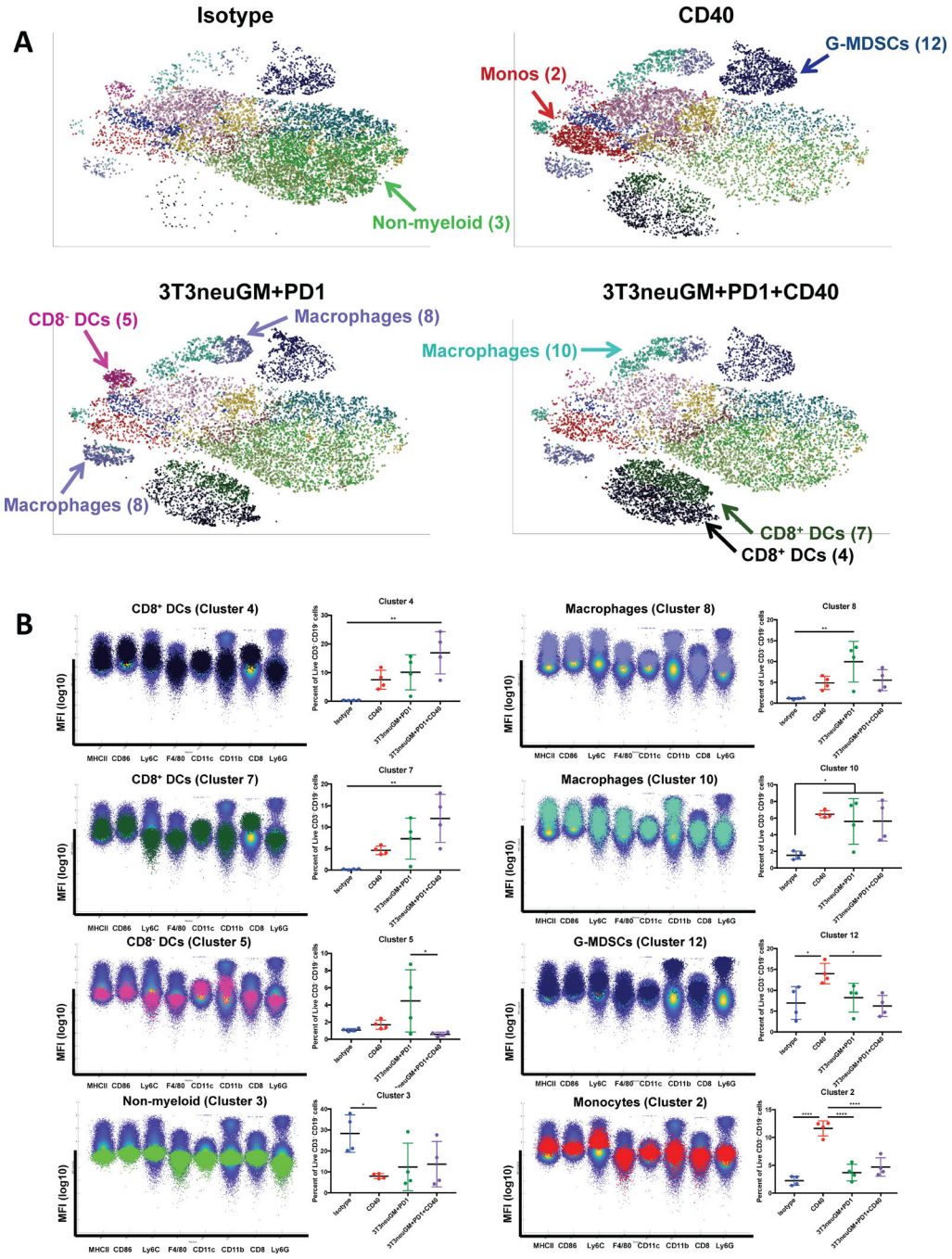

Figure 6. Triple therapy alters the myeloid component of the TME.

A) t-SNE plots of myeloid cell clusters from tumors of *neu*-N mice, separated by treatment group. Samples were gated on Live/CD3^{-}CD19^{-} cells (n = 4 mice per group). Key clusters are labeled with myeloid cell phenotype and cluster number. B) High dimensional flow plots showing MFI of each myeloid cell marker, with clusters highlighted according to cluster color and overlaid on total cells. Dot plots show frequency of each cluster per treatment group, represented by percent of Live/CD3^{-}CD19^{-} cells. *, p<0.05, **, p<0.01, ***,

p<0.001, ****, p<0.0001. t-SNE = t-distributed stochastic neighbor embedding. MFI = mean fluorescence intensity.

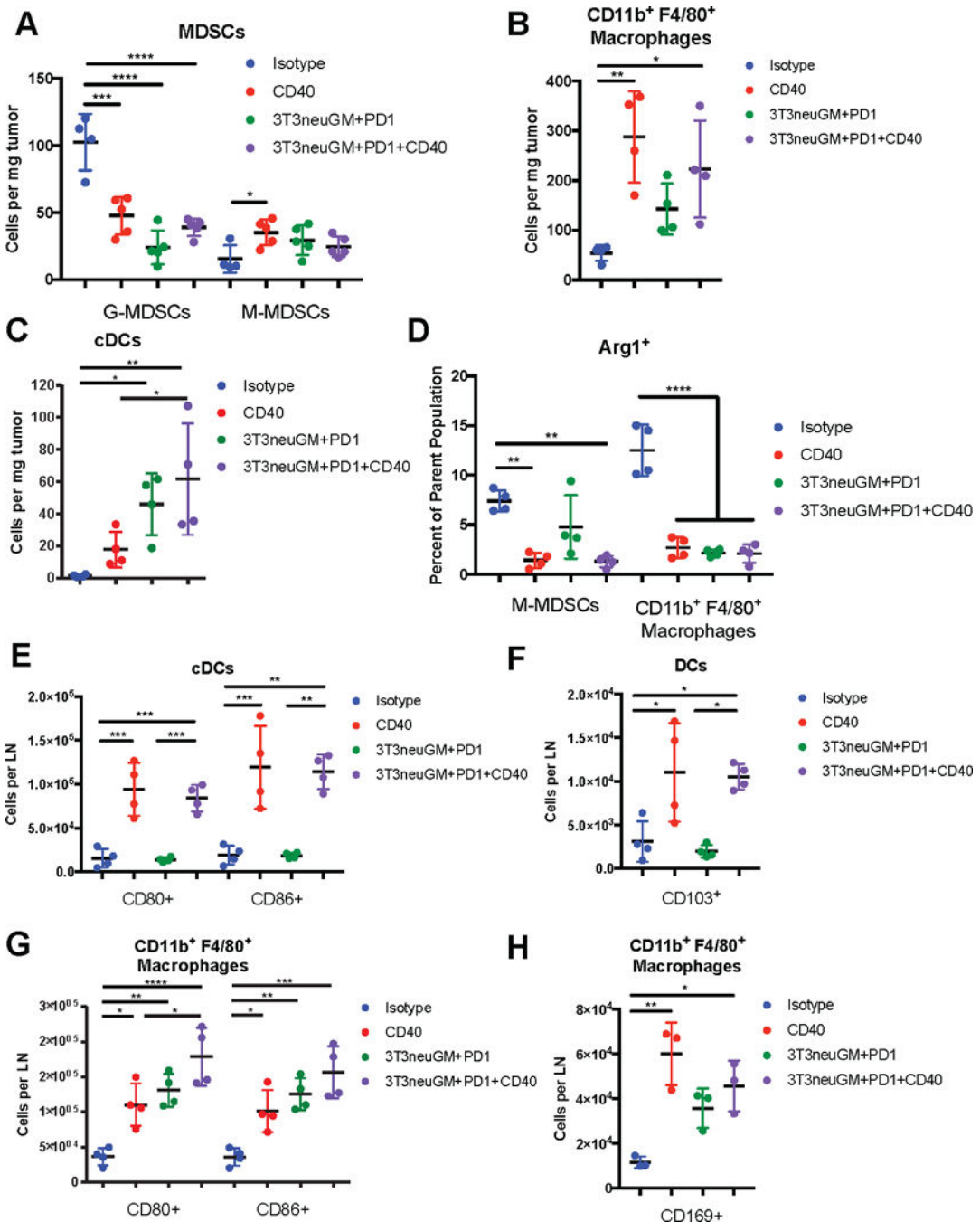

Figure 7. A CD40 agonist + vaccine + anti–PD-1 therapy alters myeloid cells in mammary tumors and TDLN.

Tumor infiltration of A) $CD11b^+$ $F4/80^-$ MDSCS ($Ly6G^+$ G-MDSCs or $Ly6C^+$ M-MDSCs), B) $CD11b^+$ $F4/80^+$ macrophages, and C) $CD8^+$ $CD11c^+$ $MHCII^+$ cDCs as measured by number of cells per mg tumor in *neu*-N mice. D) Expression of arginase 1 (Arg1) in tumor infiltrating M-MDSCs and macrophages, represented as percent of parent population. E) Expression of CD80 and CD86 in TDLN $CD11c^+$ cDCs, represented as number of positive cells per TDLN. F) $CD103^+$ DCs, represented as number of positive cells per TDLN. G) Expression of CD80 and CD86 in TDLN macrophages ($CD11b^+$ $F4/80^+$), represented as

number of positive cells per TDLN. H) $CD169^{+}$ macrophages, represented as number of positive cells per TDLN. *, $p<0.05$, **, $p<0.01$, ***, $p<0.001$, ****, $p<0.0001$.